Image denoising algorithms using norm minimization techniques

Diffellah Nacira
Dept. of electronics
(Faculty of technology)
ETA Laboratory
University of Bordj Bou Arreridj
Bordj Bou Arreridj 34000, Algeria
diffellahn@gmail.com
ORCID iD is 0000-0003-2474-0700

Bekkouche Tewfik
Dept. of electromechanics
(Faculty of technology)
ETA Laboratory
University of Bordj Bou Arreridj
Bordj Bou Arreridj 34000, Algeria
bekkou66@hotmail.com
ORCID iD is 0000-0002-5405-7382

Hamdini Rabah
Dept. of automatics
(Faculty of technology)
SET Laboratory
univ Saad Dahlab Blida
Blida 09000, Algeria
hamdinirabah@gmail.com
ORCID iD is 0000-0003-3127-1367

***Abstract*—Image denoising is one of the fundamental image processing problems. Noise removal is an important step in the image restoration process. In this paper, firstly we develop and implement two different image denoising algorithms based on norm minimization, namely ℓ_1 and ℓ_2-regularization applied to images contaminated by gaussian noise. Then, after their discretization and implementation, we perform a comparison between the two methods using several test images. Through this study, the algorithm which minimizes ℓ_2-norm of gradient of image has a unique solution and it's easy to implement, but it doesn't accept contour discontinuities, causing the obtained solution to be smooth. The ℓ_2-norm will blur the edges of the image. In order to preserve sharp edges, ℓ_1-norm is introduced. There are different methods to solve the problem of energy minimization. In this work, we have chosen the discretization finite difference method before applying the gradient descent algorithm to optimize the signal (2D grayscale images) denoising functionality.**

Experiments results, show that ℓ_1 regularization encourages image smoothness while allowing for presence of jumps and discontinuities, a key feature for image processing because of the importance of edges in human vision.

***Index Terms*—Denoising, ℓ_1-norm, ℓ_2-norm, Finite difference discretization,**

I. Introduction

In image acquisition systems, acquired digital images always contain noise. There are different kinds of digital image noise which are caused by many factors. In this paper, we focus our research to study, implement and compare two methods based on partial differential equation (PDE) model for removing Gaussian noise. Generally, images are corrupted with additive white Gaussian noise during acquisition e.g. sensor noise caused by poor illumination and/or high temperature, and/or transmission e.g. electronic circuit noise.

In the literature, several methods have been proposed to remove the noise and recover the true image u, such as iterative median filtering [1], Weight Median Filter (WMF) [2], Adaptive Median Filter (AMF) [3] [4], Wavelet Transform (WT) [5], Anisotropic diffusion filtering [6], [7] , Total Variation (TV) filter [8]–[10],...

There are many mathematical models which have been proposed to solve image denoising problems. we consider two types of image denoising problems which are expressed as the following norm minimization problems:

$$\min_{u\in V}\left\{\frac{1}{2}\|u-f\|^2+\lambda\frac{1}{2}\|\nabla u\|_2^2\right\} \tag{1}$$

$$\min_{u\in V}\left\{\frac{1}{2}\|u-f\|^2+\lambda\|\nabla u\|_1\right\} \tag{2}$$

V is the space of images (a space of smooth functions), $u\in\Re^N$ is the real image and $f\in\Re^N$ is the image contaminated by additive noise, $\lambda>0$ is regularization parameter, $\|.\|_2$ and $\|.\|_1$denotes the ℓ_2 and ℓ_1-norm , respectively. The first terms of $J_1(u,f)=\|u-f\|_2^2$ is called the data-fitting (the fidelity) term which forces the final image to be not too far away from the initial image, note that the fidelity term is convex function, and the second terms such as $J_2(u)=\frac{1}{2}\|\nabla u\|_2^2$ and $J_2(u)=\|\nabla u\|_1$ are called the regularization (or penalty) terms, which perform actually the noise reduction and they are also convex . The minimization problem (1) is called the ℓ_2-norm problem (Tikhonov regularization) and (2) is called the ℓ_1-norm regularization problem.

The rest of the paper is organized as follows: The second section presented the noise model. Section III is dedicated to analyze and implement the two different image denoising algorithms based on energy minimization: ℓ_1 and ℓ_2-regularization. In section IV, we provide some numerical experiments. Lastly, section V concludes the paper.

II. Noise model

Probability Density Function (PDF) or Histogram is also used to design and characterize the noise models, in this paper we will discuss only Gaussian noise model in digital images. Gaussian noise is statistical noise having a probability distribution function (PDF) equal to that of the normal distribution, which is also known as the Gaussian distribution. The probability density function of a Gaussian random variable is given by :

$$p_G(z)=\frac{1}{\sigma\sqrt{2\pi}}.e^{-\frac{(z-\mu)^2}{2.\sigma^2}} \tag{3}$$

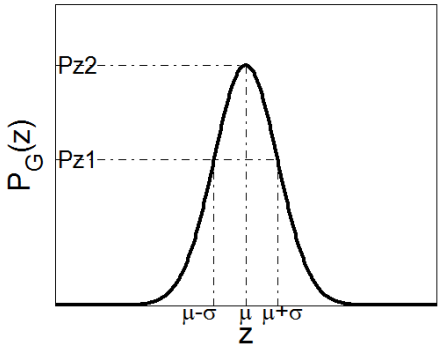

Fig. 1: Probability density function of Gaussian noise

where z represents the grey level, μ the mean value and σ the standard deviation.

The PDF of this noise model Fig. 1 shows that to noisy pixel values of degraded image in between $\mu - \sigma$ and $\mu + \sigma$. (see [11]) where

$$Pz_1 = \frac{0,607}{\sqrt{2\pi\sigma^2}} \tag{4}$$

$$Pz_2 = \frac{1}{\sqrt{2\pi\sigma^2}} \tag{5}$$

III. Methods analysis and implementation

The image denoising problem can be formulated as the following. Given an observed image f, we know f is the addition of the ideal image u and some noise with mean 0 and variance σ^2.

$$f = u + \eta \tag{6}$$

In accordance with Eq. (6), the denoising problem can be considered in the unconstrained form as:

$$J(u) = J_1(u, f) + \lambda J_2(u) \tag{7}$$

Minimization of $J_2(u)$ is equivalent to minimization of the majority of derivative over the dimension of the function. Intuitively, minimization problem (7), simultaneously try to remove the noise from the continuous image u (which is equivalent to minimization of the total first derivative over the domain) and forces the function $J_1(u)$ to be near enough to f. See [8], [12], [13].

A. Removal noise by ℓ_2- norm

The ℓ_2 norm method is a 5 steps process:

- Step 1: Create the energy that describe the quality image u

$$\min_{u\in V} J(u) = \min_{u\in V}\left\{\frac{1}{2}\|u-f\|^2 + \lambda\frac{1}{2}\|\nabla u\|^2\right\} \tag{8}$$

with

$$J_1(u) = \frac{1}{2}\|u-f\|^2 \tag{9}$$

$$J_2(u) = \frac{1}{2}\|\nabla u\|_2^2 \tag{10}$$

- Step 2: Compute the first variation of energy ∇J

$$\nabla J_1(u) = u - f \tag{11}$$

$$\nabla J_2(u) = \Delta u \tag{12}$$

so,

$$\nabla J(u) = u - f + \lambda.\Delta u \tag{13}$$

- Step 3: Setup the PDE describing the steepest descent minimization $\frac{\partial u}{\partial t} = -\nabla J$

$$\frac{\partial u}{\partial t} = -(u - f + \lambda.\Delta u) \tag{14}$$

- Step 4: Discretize the PDE in Eq. (14) by finite difference method

$$\frac{u_{i,j}^{n+1} - u_{i,j}^n}{\tau} = -\left(u_{i,j}^n - f_{i,j}^n + \lambda.D_{\ell_2}{}_{i,j}^n\right) \tag{15}$$

with

$$\Delta u \overset{\text{discretization}}{\rightarrow} D\ell_2{}_{i,j}^n \tag{16}$$

$$D\ell_2{}_{i,j}^n = u_{i-1,j}^n + u_{i+1,j}^n + u_{i,j-1}^n + u_{i,j+1}^n - 4u_{i,j}^n \tag{17}$$

- Step 5: Evolve the PDE towards the minimum of

$$u_{i,j}^{n+1} = u_{i,j}^n - \tau\left(u_{i,j}^n - f_{i,j}^n + \lambda D\ell_2{}_{i,j}^n\right) \tag{18}$$

B. Removal noise by ℓ_1- norm

The ℓ_1 norm method is a 5 steps process:

- Step 1: Create the energy that describe the quality image u

$$\min_{u\in V} J(u) = \min_{u\in V}\left\{\frac{1}{2}\|u-f\|^2 + \lambda\|\nabla u\|_1\right\} \tag{19}$$

with

$$J_1(u) = \frac{1}{2}\|u-f\|^2 \tag{20}$$

$$J_2(u) = \|\nabla u\|_1 \tag{21}$$

- Step 2: Compute the first variation of energy ∇J

$$\nabla J_1(u) = u - f \tag{22}$$

$$\nabla J_2(u) = div\frac{\nabla u}{\|\nabla u\|} \tag{23}$$

so,

$$\nabla J(u) = u - f + \lambda.div\frac{\nabla u}{\|\nabla u\|} \tag{24}$$

- Step 3: Setup the PDE describing the steepest descent minimization $\frac{\partial u}{\partial t} = -\nabla J$

$$\frac{\partial u}{\partial t} = -\left(u - f + \lambda.div\frac{\nabla u}{\|\nabla u\|}\right) \tag{25}$$

- Step 4: Discretize the PDE in Eq. (25) by finite difference method

$$\frac{u_{i,j}^{n+1} - u_{i,j}^n}{\tau} = -\left(u_{i,j}^n - f_{i,j}^n + \lambda.D_{\ell_1}{}_{i,j}^n\right) \tag{26}$$

with

$$div\left(\frac{\nabla u}{\|\nabla u\|}\right) \overset{\text{discretization}}{\rightarrow} D\ell_1{}_{i,j}^n \tag{27}$$

$$D{\ell_1}^n_{i,j} = \frac{1}{h^2}\left[\frac{d^n_{1_{i,j}}}{c^n_{1_{i,j}}} - \frac{d^n_{2_{i,j}}}{c^n_{2_{i,j}}} + \frac{d^n_{3_{i,j}}}{c^n_{3_{i,j}}} - \frac{d^n_{4_{i,j}}}{c^n_{4_{i,j}}}\right] \quad (28)$$

$$c^n_{1_{i,j}} = \sqrt{\varepsilon^2 + \left(\frac{d^n_{1_{i,j}}}{h^2}\right)^2 + \left(\frac{u_{i,j+1} - u_{i,j-1}}{2h}\right)^2} \quad (29)$$

$$c^n_{2_{i,j}} = \sqrt{\left(\frac{d^n_{2_{i,j}}}{h^2}\right)^2 + \left(\frac{u_{i-1,j+1} - u_{i-1,j-1}}{2h}\right)^2} \quad (30)$$

$$c^n_{3_{i,j}} = \sqrt{\left(\frac{u_{i+1,j} - u_{i-1,j}}{2h}\right)^2 + \left(\frac{d^n_{3_{i,j}}}{h^2}\right)^2} \quad (31)$$

$$c^n_{4_{i,j}} = \sqrt{\left(\frac{u_{i+1,j-1} - u_{i-1,j-1}}{2h}\right)^2 + \left(\frac{d^n_{4_{i,j}}}{h^2}\right)^2} \quad (32)$$

$$d^n_{1_{i,j}} = u^n_{i+1,j} - u^n_{i,j} \quad (33)$$

$$d^n_{2_{i,j}} = u^n_{i,j} - u^n_{i-1,j} \quad (34)$$

$$d^n_{3_{i,j}} = u^n_{i,j+1} - u^n_{i,j} \quad (35)$$

$$d^n_{4_{i,j}} = u^n_{i,j} - u^n_{i,j-1} \quad (36)$$

- Step 5: Evolve the PDE towards the minimum of

$$u^{n+1}_{i,j} = u^n_{i,j} - \tau\left(u^n_{i,j} - f^n_{i,j} + \lambda D{\ell_1}^n_{i,j}\right) \quad (37)$$

IV. Numerical results

In this section, we will compare and discuss the results of the different algorithms. Our implementation of the two algorithms has been tested against the set of images: cameraman of size 256×256 pixels, Einstein 1064×948 pixels, Tower 474×422 pixels and Lena 512×512 pixels shown in Fig. 2a , Fig. 3a, Fig. 4a and Fig. 5a respectively.

As a measure of quality, we use three metrics, namely , Signal Noise to Ratio $SNR\,[dB]$, Peak Signal-to-Noise Ratio (PSNR) and Structural SIMilarity index (SSIM) [14].

- The Signal Noise to Ratio $SNR\,[dB]$ is defined as:

$$SNR = \frac{S_A - S_B}{\partial_0} \quad (38)$$

S_A is the original image and S_B is the restored noisy image, σ_0 is standard deviation of the image.
This measure of SNR is useful in giving an indication of the noise in an image, but the exact visual effect of such noise is highly image dependent.

- The PSNR metric is defined as:

$$PSNR\,(u, \hat{u}) = 10 \log \frac{{L_d}^2}{MSE} \quad (39)$$

where L_d is the dynamic range of the pixel-values. If the input image has an 8-bit unsigned integer data type, $L_d = 255$.
Equation 40 give the expression of the quality measures Mean Squared Error (MSE):

$$MSE\,(u, \hat{u}) = \frac{1}{M \times N}\sum_{i=1}^{M}\sum_{j=1}^{N}\left(u\,(i,j) - \hat{u}\,(i,j)\right)^2. \quad (40)$$

$u\,(i,j)$ denote the original image and $\hat{u}\,(i,j)$ its reconstructed image, respectively. M and N are the image size. PSNR determines the degradation in the embedded image with respect to the original image. PSNR is more consistent in the presence of noise compared to SNR. The main advantages of PSNR are that it is very fast and easy to implement. The value of PSNR is larger, indicating that denoising effect is better.

- The mathematical representation of the SSIM is as follows:

$$SSIM\,(u, \hat{u}) = \frac{(2\mu_u\mu_{\hat{u}} + C_1)\,(2\sigma_{u\hat{u}} + C_2)}{(\mu_u^2 + \mu_{\hat{u}}^2 + C_1)\,(\sigma_u^2 + \sigma_{\hat{u}}^2 + C_2)} \quad (41)$$

where

$$\mu_u = \frac{1}{N}\sum_{i=1}^{N} u_i \quad (42)$$

$$\mu_{\hat{u}} = \frac{1}{N}\sum_{i=1}^{N} \hat{u}_i \quad (43)$$

$$\sigma_u = \sqrt{\frac{1}{N-1}\sum_{i=1}^{N}\left(u_i - \mu_u\right)^2} \quad (44)$$

$$\sigma_{\hat{u}} = \sqrt{\frac{1}{N-1}\sum_{i=1}^{N}\left(\hat{u}_i - \mu_{\hat{u}}\right)^2} \quad (45)$$

$$\sigma_{u\hat{u}} = \frac{1}{N-1}\sum_{i=1}^{N}\left(u_i - \mu_u\right)\left(\hat{u}_i - \mu_{\hat{u}}\right) \quad (46)$$

μ_u and $\mu_{\hat{u}}$ are the means and variances of u and $\hat{u}$ respectively.
σ_u^2 and $\sigma_{\hat{u}}^2$ are variances of u and $\hat{u}$ respectively.
$\sigma_{u\hat{u}}$ is the standard deviation between u and $\hat{u}$.
C_1 and C_2 are constants which are used to avoid instability when $\mu_u^2 + \mu_{\hat{u}}^2$ and $\sigma_u^2 + \sigma_{\hat{u}}^2$ are very close to zero.

$$C_1 = \left(K_1 L_d\right)^2 \quad (47)$$

$$C_2 = \left(K_2 L_d\right)^2 \quad (48)$$

K_1 and K_2 are two scalar constants given by; $K_1 = 0.01$ and $K_2 = 0.03$.
$SSIM$ satisfies the following conditions:

- $SSIM\,(u, \hat{u}) = SSIM\,(\hat{u}, u)$
- $SSIM\,(u, \hat{u}) \leq 1$
- $SSIM\,(u, \hat{u}) = 1\ si\ \hat{u} = u$

(a) True image

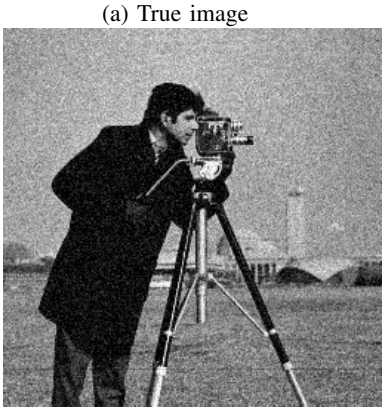

(b) Noisy image $\sigma = 20$

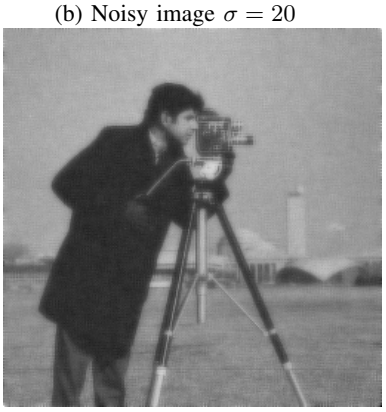

(c) ℓ_2-norm

(d) ℓ_1-norm

Fig. 2: Removal noise applied to 'Cameraman'

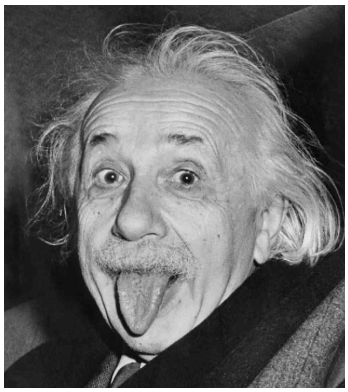

(a) True image

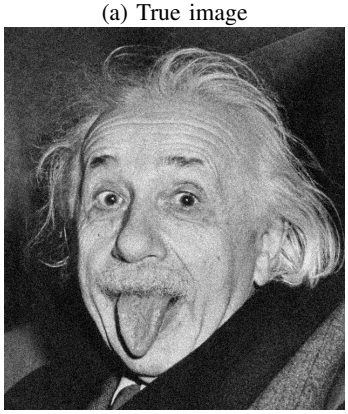

(b) Noisy image

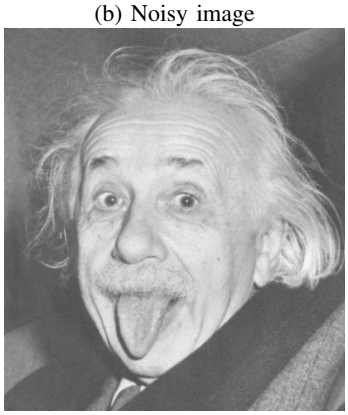

(c) ℓ_2-norm

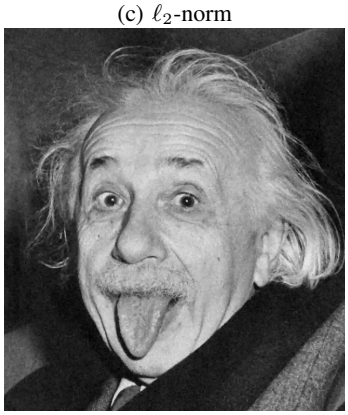

(d) ℓ_1-norm

Fig. 3: Removal noise applied to 'Eistein'

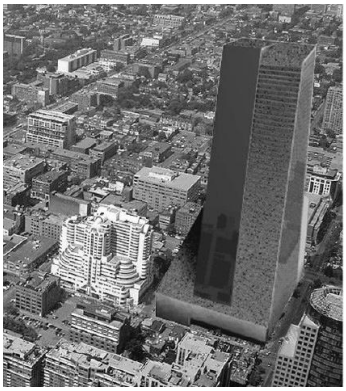

(a) True image

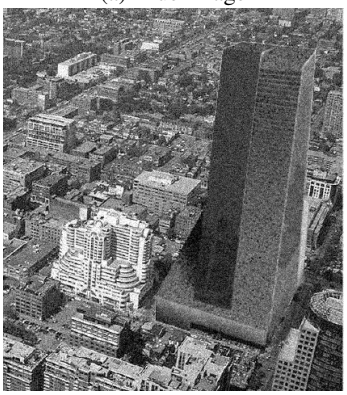

(b) Noisy image $\sigma = 20$

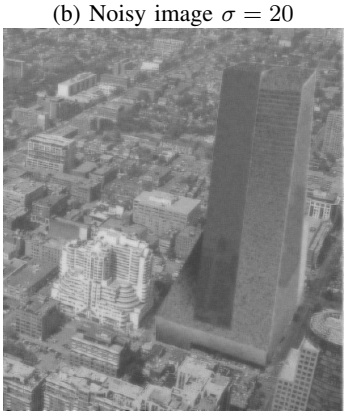

(c) ℓ_2-norm

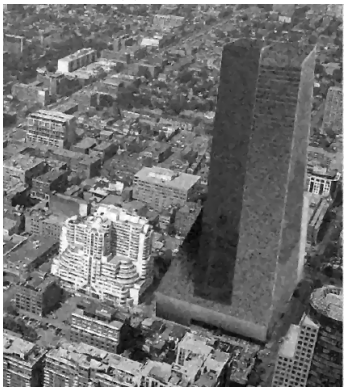

(d) ℓ_1-norm

Fig. 4: Removal noise applied to 'Tower'

(a) True image

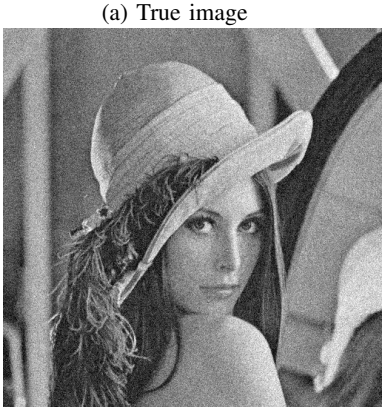

(b) Noisy image $\sigma = 20$

(c) ℓ_2-norm

(d) ℓ_1-norm

Fig. 5: Removal noise applied to 'lena'

SSIM compares two images using information about luminous, contrast and structure, it's decimal value is between $[-1, 1]$.

Images corrupted by Gaussian noise are shown in Fig. 2b, Fig. 3b, Fig. 4b and Fig. 5b. The results using ℓ_1-norm regularization and images denoised with ℓ_2-norm regularization are shown in Fig. 2d, Fig. 3d, Fig. 4d, Fig. 5d and Fig. 2c, Fig. 3c, Fig. 4c and Fig. 5c.

Obtained results of SNR, PSNR and SSIM for the two proposed algorithms are summarized in Tables I, II and III, respectively.

TABLE I: Comparison of the denoising SNR results

Image	ℓ	σ					
		10	20	30	50	70	100
Camera-man	ℓ_1	16.91	15.55	12.83	7.36	3.33	-0.73
	ℓ_2	15.86	11, 60	6.31	1.92	-0.99	-4.09
Einstein	ℓ_1	21.82	19.54	14.83	8.05	3.82	-0.42
	ℓ_2	16.15	11, 19	6.61	2.17	-0.74	-3.84
Tower	ℓ_1	9.93	9, 33	8.02	4.56	1.22	-2.60
	ℓ_2	13.93	4, 92	4.34	-0.05	-2.99	-6.09
Lena	ℓ_1	18.48	16.08	11.83	5.39	1.23	-2.98
	ℓ_2	13.61	10, 36	4.07	-0.37	-3.30	-6.41

TABLE II: Comparison of the denoising $PSNR$ results

Image	ℓ	σ					
		10	20	30	50	70	100
Cameraman	ℓ_1	29.14	27.82	25.06	19.60	15.57	11.50
	ℓ_2	28.10	22.11	18.55	14.16	11.23	8.14
Einstein	ℓ_1	33.82	31.53	26.83	20.05	15.81	11.57
	ℓ_2	28.12	22.11	18.58	14.14	11.22	8.12
Tower	ℓ_1	23.85	23.27	21.94	18.48	15.14	11.31
	ℓ_2	28.14	22.08	18.56	14.16	11.22	8.12
Lena	ℓ_1	33.01	30.59	26.36	19.92	15.76	11.54
	ℓ_2	28.14	22.11	18.60	14.15	11.22	8.12

TABLE III: Comparison of the denoising $SSIM$ results

Image	ℓ	σ					
		10	20	30	50	70	100
Cameraman	ℓ_1	0.85	0.78	0.57	0.30	0.19	0.11
	ℓ_2	0.63	0.39	0.28	0.17	0.12	0.07
Einstein	ℓ_1	0.96	0.92	0.83	0.64	0.50	0.36
	ℓ_2	0.96	0.88	0.78	0.61	0.48	0.35
Tower	ℓ_1	0.90	0.88	0.81	0.68	0.54	0.39
	ℓ_2	0.95	0.86	0.76	0.59	0.46	0.33
Lena	ℓ_1	0.94	0.88	0.71	0.46	0.32	0.20
	ℓ_2	0.87	0.67	0.53	0.35	0.25	0.16

The ℓ_1 method has significantly better reconstruction results, both in terms of SNR, $PSNR$, $SSIM$ and visual quality than the ℓ_2 method.

V. Conclsuion

To denoise image corrupted with Gaussian noise, we have studied and implemented two algorithms regularization schemes ℓ_1 and ℓ_2. The ℓ_2 regularization scheme does not have edge preserving properties, but is capable of removing almost all the noise from the image, but the ℓ_1 regularization scheme is capable of removing noise and also preserving edges to a large extent.

Finally, we confirm through experimental results that the ℓ_1 regularization problem involved by Eq. (2) restore the true image better than ℓ_2 regularization problem expressed by Eq. (1).

For future works, there are many aspects need to be investigated. For example, minimizing the energy function using a variational method and deep learning-based methods.

Acknowledgements

The authors would like to thank the organizers of the conference ICCSA'2021 and the anonymous reviewers for their valuable comments and suggestions which greatly improved the quality of the paper. Authors would like to thank too the General Directorate for Scientific Research and Technological Development of the Algerian Republic in general and the ETA research laboratory of Bordj Bou Arreridj University in particular, for all material and financial support to accomplish this work.

References

[1] J. Nichol and V.Vohra, "Noise over water surfaces in landsat tm images," *International Journal of Remote Sensing*, vol. 25, no. 11, pp. 2087–2093, 2004.

[2] F. N. Hasson, "Weight median filter using neural network for reducing impulse noise," Ph.D. dissertation, Department Computer Sciences, University of Putra,Putra, Malaysia, 2004.

[3] D. Dhanasekaran, A. Krishnamurthy, and J. Ramkumar, "High speed pipeline architecture for adaptive median filter," *Journal of Scientific Research*, vol. .29, no. 4, pp. 454–460, 2009.

[4] R. C. Gonzalez and R. E. Woods, *Digital Image Processing*, 4th ed., Pearson, Ed., 2018.

[5] M. Longkumer and H. Gupta, "Image denoising using wavelet transform,median filter and soft threshoding," *International Research Journal of Engineering and Technology (IRJET)*, vol. 5, no. 7, pp. 729–732, 2018.

[6] N. K. Gill and A. Sharma, "Noise models and de-noising techniques in digital image processing," *International Journal of Computer & Mathematical Sciences IJCMS*, vol. 5, pp. 21–25, 2016.

[7] W. S. abd Min Han, "Adaptive search based non-local means image denoising," *2nd International Congress on Image and Signal Processing CISP*, vol. 9, pp. 1–4, 2009.

[8] L. I.Rudin, S. Osher, and E. Fatemi, "Nonlinear total variation based noise removal algorithms," *Physica D: Nonlinear Phenomena*, vol. 60, pp. 259–268, 1992.

[9] A. Chambolle, "An algorithm for total variation minimization and applications," *Journal of Mathematical Imaging and Vision*, vol. 20, pp. 89–97, 2004.

[10] D. N. H. Thanh, L. T. Thanh, N. N. Hien, and S. Prasath, "Adaptative tototal variation l1 regularization for salt and pepper image denoising," *Optik*, vol. 208, no. 208, 2020.

[11] W. Bryc, *The Normal Distribution Characterizations with Applications*. Springer-Verlag New York, 1995, no. 1.

[12] F. Alter, V. Caselles, and A. Chambolle, "Evolution of characteristic functions of convex sets in the plane by the minimizing total variation flow," *Interfaces and Free Boundaries*, vol. 7, no. 1, pp. 29–53, 2005.

[13] A. Chambolle and T. Pock, "A first-order primal-dual algorithm for convex problems with applications to imaging," *Journal of Mathematical Imaging and Vision*, vol. 40, pp. 120–145, 2011.

[14] Z. Wang, A. Bovik, H. Sheikh, and E. Simoncelli, "Image quality assessment: from error visibility to structural similarity," *IEEE Transactions on Image Processing*, vol. 13, no. 4, pp. 600 – 612, 2004.